Earth Planet. Sci. Lett. 671 (2025) 119688

Contents lists available at ScienceDirect

Earth and Planetary Science Letters

journal homepage: www.elsevier.com/locate/epsl

High-precision geochronology of the Early Cretaceous Jiufotang Formation: Temporal constraints on the late phase of the Jehol Biota

Yu-Ting Zhong [a], Magdalena H. Huyskens [b,1], Run-Jian Chu [c], Han-Qing Yang [a], Jian-Fang Hu [a], Ya-Qiong Wang [d], Shi-Xi Cai [a], Qiong Wu [e], Qiang Ma [f], Huai-Chun Wu [c], Qing-Zhu Yin [b], Yi-Gang Xu [a,*]

[a] State Key Laboratory of Deep Earth Processes and Resources, Guangzhou Institute of Geochemistry, Chinese Academy of Sciences, Guangzhou 510640, China
[b] Department of Earth and Planetary Sciences, University of California-Davis, Davis, CA 95616, USA
[c] State Key Laboratory of Geomicrobiology and Environmental Changes, China University of Geosciences, Beijing 100083, China
[d] State Key Laboratory of Palaeobiology and Stratigraphy, Nanjing Institute of Geology and Palaeontology, Chinese Academy of Sciences, Nanjing 210008, China
[e] Southern Marine Science and Engineering Guangdong Laboratory (Guangzhou), Guangzhou 511458, China
[f] State Key Laboratory of Geological Processes and Mineral Resources, School of Earth Sciences, China University of Geosciences, Wuhan 430074, China

ARTICLE INFO

Editor: Dr A Webb

ABSTRACT

The Lower Cretaceous Jiufotang Formation in western Liaoning, northeastern China, hosts exceptionally preserved fossils that represent the late phase of the Jehol Biota, a key Early Cretaceous terrestrial ecosystem. However, its temporal framework has remained poorly constrained. This study combines high-precision U-Pb geochronology, Bayesian age modeling, and cyclostratigraphy based on core data from the Yixian-Jiufotang succession to refine its chronology. The Yixian/Jiufotang formation boundary is dated to 124.44 ± 0.29 Ma, with the Jiufotang Formation deposited between 124.44 and 112.25 Ma, spanning 12.2 Myr from the Early Barremian to Early Albian. Sedimentation in the Jiufotang Formation was relatively stable at 8–16 cm/kyr, reflecting rift-related sustained subsidence and development of large lakes. Well preserved fossiliferous layers are precisely dated to 121.09+0.18/-0.75 Ma (Shangheshou, Chaoyang Basin) and 121.539 ± 0.085 Ma (Xiaotaizi, Jianchang Basin), constraining the late phase of the Jehol Biota to ~124–121 Ma—~1 Myr shorter than previous estimates. Additionally, widespread black shales in the Jiufotang Formation record enhanced organic carbon burial during the Aptian cold interval, indicating major carbon cycle perturbations. This refined chronostratigraphic framework improves the temporal calibration of the Jiufotang Formation and the late phase of the Jehol Biota.

1. Introduction

The Jehol Biota represents a terrestrial ecosystem of the Early Cretaceous and is mainly found in northern China, especially in western Liaoning, northern Hebei and southeastern Inner Mongolia. It is well known for exceptionally preserved fossils, including early birds, feathered dinosaurs, primitive mammals, and a variety of plants such as early angiosperms. These fossils offer critical insights into Mesozoic terrestrial evolution (Zhou et al., 2003). The Jehol Biota is generally divided into three stages, referred to as Jehol Biota stages I to III (JBS I to III), corresponding to the fossil assemblages from the Huajiying, Yixian, and Jiufotang formations, respectively (Zhou et al., 2021; Fig. 1). Among them, the vertebrate fossils from the Jiufotang Formation show remarkable differentiation (Zhou, 2014). Volcanic tuffs interbedded within these fossiliferous sequences enable radiometric dating and have helped construct a chronological framework that spans roughly from 135 to 120 Ma (e.g., Swisher et al., 2002; He et al., 2004; Yang et al., 2020). For instance, Yang et al. (2020) constrained the age of the Huajiying Formation to ~135–127 Ma, which helps clarify the evolutionary timing of the JBS I. Recent high-precision dating studies have established the duration of JBS II (Yixian Formation) to be ~126–124 Ma (Zhong et al., 2021; Li et al., 2022; MacLennan et al., 2024). These precise age constraints improve our understanding of evolutionary rates by refining previous duration estimates. In contrast, the age of JBS III

* Corresponding author.
E-mail address: yigangxu@gig.ac.cn (Y.-G. Xu).
1 Current address: Geological Survey of Norway, Leiv Eirikssons vei 39, 7040 Trondheim, Norway.

https://doi.org/10.1016/j.epsl.2025.119688
Received 20 June 2025; Received in revised form 23 September 2025; Accepted 11 October 2025
Available online 16 October 2025

(Jiufotang Formation) remains less well defined, with existing dates broadly spanning 124–120 Ma (e.g., He et al., 2004; Yu et al., 2021). Precise age determinations for key fossil-bearing horizons in this formation are still lacking, and a consensus on the temporal framework has not been reached. This uncertainty hinders our understanding of the evolutionary history of the Jehol Biota and its spatiotemporal distribution patterns. Although M.D. Sun et al. (2025) constructed a high-resolution chemostratigraphic framework for the Jiufotang Formation in the Kazuo Basin, they did not provide a basal age of the formation or precise dates for major fossiliferous layers. Consequently, the timing of vertebrate radiation within the Jiufotang Formation remains poorly understood. This also hinders correlation with broader Early Cretaceous environmental changes.

To obtain continuous and unaltered samples, the Yanshan Scientific Drilling Project drilled a core (YSDP-1) at the Chaoyang Bird Fossil National Geological Park (41°36′02″N, 120°22′40″E) in the Chaoyang Basin, western Liaoning (Fig. 1a). In this study, we present high-precision U-Pb ages from four tuff/tuffaceous layers sampled from the YSDP-1 core. These ages combined with a Bayesian age modeling and cyclostratigraphic analysis to establish a high-resolution chronostratigraphic framework for the Jiufotang Formation in the Chaoyang Basin. Additionally, we provide precise age constraints on two exceptionally preserved fossiliferous layers within the Jiufotang Formation, namely the Shangheshou and Xiaotaizi sections, respectively. Through correlation with the chemostratigraphic data from the Kazuo Basin (Fig. 2d), we have achieved regional chronostratigraphic consistency for the Jiufotang Formation.

2. Geological setting and samples

The eastern North China Craton (NCC) experienced significant development of rift basins from the Middle Jurassic to the Early Cretaceous. Late Mesozoic NNE- to NE-oriented rift basins in Western Liaoning lie along the northern margin of the eastern NCC (Zhou et al., 2021). The lower Cretaceous Yixian and Jiufotang formations are distributed across four basins, from northwest to southeast, the Lingyuan-Sanshijiazi Basin, Chaoyang-Kazuo Basin, Jianchang Basin, and Fuxin-Yixian-Jinzhou Basin (Jiang and Sha, 2006; Fig. 1a). In the Chaoyang Basin, the Lower Cretaceous succession includes the Yixian, Jiufotang, Shahai-Fuxin, and Sunjiawan formations in ascending order (Fig. 1). The Jiufotang Formation, ranging from 206 to 2685 m, increasing gradually from the eastern basins towards the western basins, and primarily consisting of mudstone, siltstone, shale, sandstone and tuff (Sha, 2007).

The YSDP-1 borehole was drilled near (<100 m) the well-known Shangheshou section (Fig. 1a), a significant fossil site in the Jiufotang Formation that contains abundant fossils of birds, dinosaurs, pterosaurs, and aquatic fauna (He et al., 2004). The 429.7-m core recovered: (1) 1 m of Quaternary topsoil; (2) 283.5 m of Jiufotang Formation (~1–284.5 m); and (3) 142.5 m of underlying volcanic rocks assigned to the underlying Yixian Formation (284.5–429.7 m). The 17–47 m interval, characterized by black shale interbedded with sandstone and several tuff layers along with fossils, correlates with the main fossiliferous horizon of the Shangheshou section (He et al., 2004; Meng, 2008). Detailed descriptions of the core are available in S. Cai et al. (2025).

U-Pb age sampling focused on tuff layers and boundary-critical horizons, including three tuff samples (CYZK-16, 53.06–53.26 m; CYZK-22, 155.01–155.13 m; CYZK-45, 306.14–306.27 m), and one tuffaceous sandstone (CYZK-41, 283.53–283.73 m) collected from within 1 m above the boundary of the Yixian/Jiufotang formations to better constrain this previously unresolved basal boundary (Figs. 2b and S1). Additionally, tuff sample JC17–3 collected above the fossil-bearing shale layer of the Xiaotaizi section in the Jianchang Basin was analyzed to support correlation with the upper the Jiufotang Formation (Yu et al., 2021; Figs. 2c and S1). For organic carbon isotopic composition ($\delta^{13}C_{org}$) analysis, 24 samples were collected from the 1280–1330 m interval of the YSDP-4 core (M.D. Sun et al., 2025; Fig. 1a).

3. Results

3.1. High resolution U-Pb geochronology

Twenty-nine zircon grains from four tuff samples (CYZK-16, CYZK-22, CYZK-45, and JC17–30), and one tuffaceous sandstone (CYZK-41) were dated using CA-ID-IRMS (chemical abrasion-isotope dilution-isotope ratio mass spectrometry) (Figs. 2 and S2; Table S1). All age uncertainties are reported at 2σ and expressed in three levels: analytical only (X), analytical and tracer calibration (Y), and full uncertainty including decay constant (Z). The youngest coherent cluster (at least two analyses) is considered as the best estimate of depositional age. Analysis yielding younger ages are attributed to Pb loss, while older dates likely reflect inheritance.

Six grains were analyzed from sample CYZK-16, with $^{206}Pb/^{238}U$ dates ranging from 121.07 ± 0.17 Ma to 160.65 ± 0.32 Ma (Table S1).

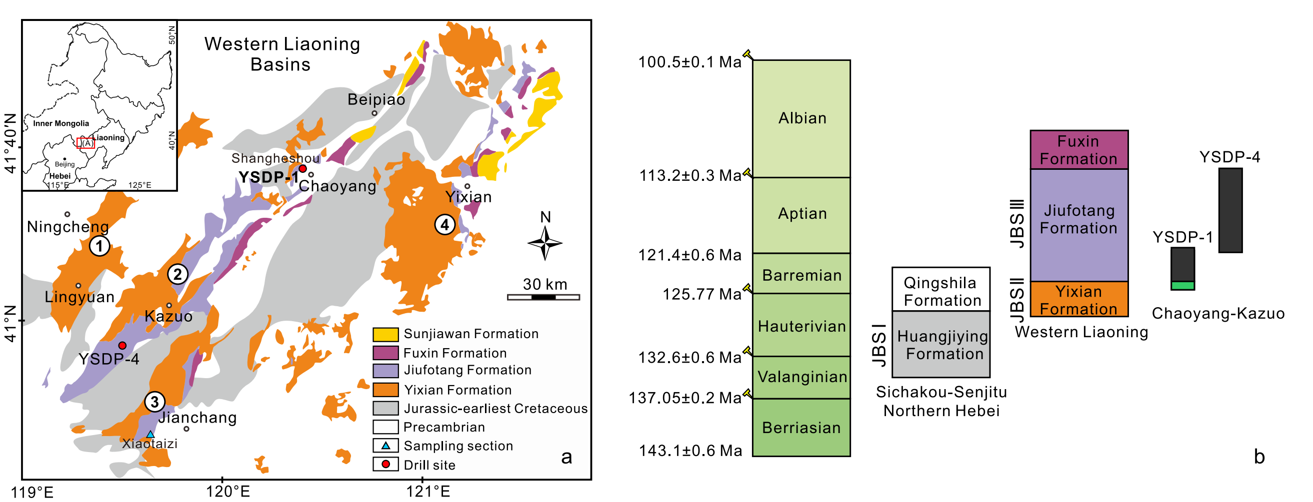

Fig. 1. (a) Simplified geological map of western Liaoning (modified from Zhong et al. (2021)). 1: Lingyuan-Sanshijiazi Basin; 2: Chaoyang-Kazuo Basin; 3: Jianchang Basin; 4: Fuxin-Yixian-Jinzhou Basin. The YSDP-1 drill site is located in the Shangheshou section, where abundant Jehol Biota fossils have been excavated. The YSDP-4 is located in the Kazuo Basin (M.D. Sun et al., 2025). (b) Chronostratigraphy of northern Hebei (Sichakou-Senjitu Basin) and western Liaoning, with stratigraphic positions of YSDP-1 and YSDP-4 cores. The Huajiying, Yixian and Jiufotang formations host the Jehol Biota, corresponding to Jehol Biota stages I to III (JBS I to III).

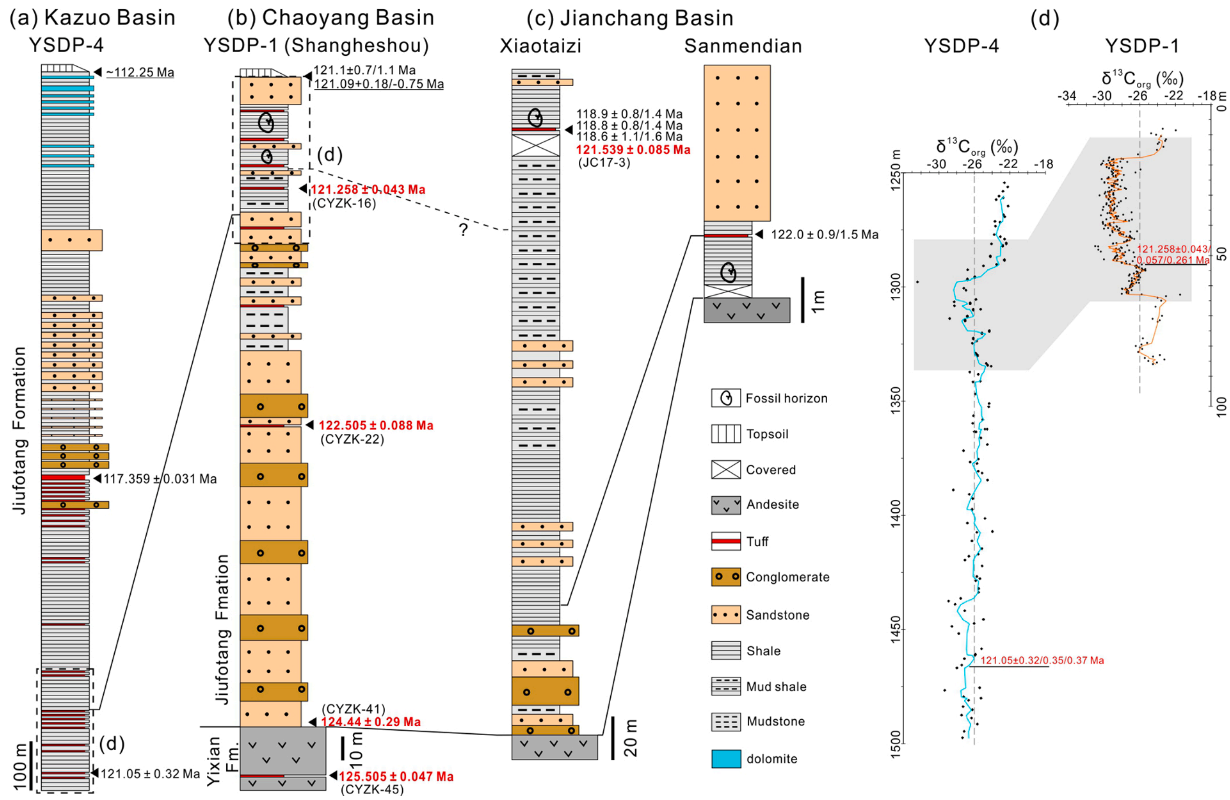

Fig. 2. Early Cretaceous stratigraphy, sampling horizons, and geochronology for (a) Kazuo Basin (YSDP-4 core), (b) Chaoyang Basin (YSDP-1 core/Shangheshou section), (c) Jianchang Basin (Xiaotaizi and Sanmendian sections) (modified from M.D. Sun et al. (2025) and Yu et al. (2021). Red bold ages denote CA-ID-IRMS results from this study; black ages are compiled from Yu et al. (2021) and M.D. Sun et al. (2025). Underlined ages were derived from Bayesian age-depth model. (d) $^{13}C_{org}$ profiles of YSDP-4 and YSDP-1. The intervals of YSDP-4 and YSDP-1 correspond to the dashed boxes in (a) and (b), respectively. $\delta^{13}C_{org}$ values are sourced from Sun M et al. (M.D. 2025), Sun Z et al. (Z. 2025) and this study. Fm–Formation.

Excluding a Jurassic outlier (160.65 Ma) and one older inherited grain, four concordant analyses define a weighted-mean $^{206}Pb/^{238}U$ date of 121.258 ± 0.043/0.057/0.261 Ma (n = 4, mean square weighted deviation (MSWD) = 3.2) (Figure S2b), interpreted as the depositional age of the tuff layer at 53.26 m of the YSDP-1 core.

Six grains were analyzed from sample CYZK-22, with $^{206}Pb/^{238}U$ dates ranging from 119.37 ± 0.15 Ma to 122.93 ± 0.30 Ma (Table S1). Two grains are considerably younger, interpreted as affected by Pb loss, and one grain is older and regarded as inherited; all three lie outside the 2σ uncertainty of the weighted-mean age. The remaining three analyses yield a weighted-mean age of 122.505 ± 0.088/0.096/0.275 Ma (n = 3, MSWD = 0.4) (Figure S2d), interpreted as the depositional age for this tuff sample at the 155.13 m depth of YSDP-1.

Six grains were analyzed from the tuffaceous sandstone (CYZK-41) at the boundary of the Yixian/Jiufotang formations, with $^{206}Pb/^{238}U$ dates ranging from 124.40 ± 0.08 Ma to 124.66 ± 0.17 Ma (Table S1). The two youngest overlapping analyses yield a weighted-mean $^{206}Pb/^{238}U$ date of 124.440 ± 0.290/0.293/0.392 Ma (n = 2, MSWD = 1.2) (Figure S2f), representing the youngest coherent cluster. This provides a maximum depositional age for the Yixian-Jiufotang transition.

Seven grains were analyzed from the tuff sample CYZK-45, with $^{206}Pb/^{238}U$ dates ranging from 125.17 ± 0.15 Ma to 125.87 ± 0.33 Ma (Table S1). One slightly younger grain is interpreted as affected by Pb loss, and two older grains are regarded as inherited. The remaining four analyses define the youngest coherent cluster and yield a weighted-mean $^{206}Pb/^{238}U$ date of 125.505 ± 0.047/0.061/0.271 Ma (n = 4, MSWD = 0.4) (Figure S2h). This date is interpreted as the depositional age of the tuff sample from the depth of 306.27 m.

Four grains were analyzed from sample JC17–3, with $^{206}Pb/^{238}U$ dates ranging from 120.95 ± 0.27 Ma to 121.57 ± 0.11 Ma (Table S1). One analysis is considerably younger and discordant, probably due to Pb loss, and is excluded from the age calculation. The remaining three analyses yield a weighted-mean age of 121.539 ± 0.085/0.093/0.272 Ma (n = 3, MSWD= 1.1) (Figure S2j), which is interpreted as the depositional age of JC17–3. This age can also be approximately regarded as the age of the exceptionally preserved fossiliferous layers of the Xiaotaizi section.

3.2. Bayesian age-depth modeling

A Bayesian Bchron age-depth model (Haslett and Parnell, 2008; Parnell et al., 2008) was established using three radiometrically constrained horizons within the YSDP-1 core (CYZK-16, CYZK-22, and CYZK-41) (Fig. 3). This statistical framework resolved two critical chronostratigraphic anchors: (1) a core top age of 121.09+0.18/−0.75 Ma, and (2) the Yixian/Jiufotang formations boundary age of 124.44+0.29/−0.30 Ma (Fig. 3). Sample CYZK-41, located <1 m above the Yixian/Jiufotang formations boundary, yields a CA-ID-IRMS U-Pb age of 124.44 ± 0.29 Ma. To avoid circular reasoning, CYZK-41 was excluded from the Bayesian model. A simple linear extrapolation using only CYZK-16 and CYZK-22 yields 124.09 ± 0.10 Ma at 284.5 m (i.e., Yixian/Jiufotang formations boundary), which is consistent within uncertainties with both the direct age of CYZK-41 age and the Bayesian model result. We therefore regard the direct U-Pb age of CYZK-41, confirmed by the independent extrapolation, as a robust chronostratigraphic marker for this boundary. This result also resolves previous ambiguities concerning the basal age of the Jiufotang Formation in regional stratigraphic frameworks (e.g., Li et al., 2023; M.D. Sun et al., 2025).

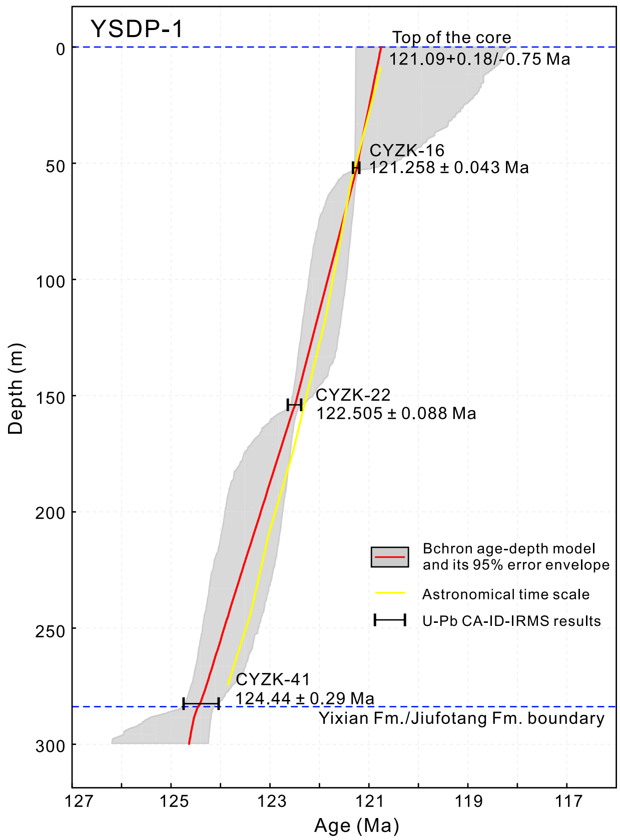

Fig. 3. U-Pb geochronological (red line) the astronomical (yellow line) age-depth models for the YSDP-1 core at Chaoyang Basin, western Liaoning. U-Pb dates are shown with their 2σ internal uncertainties. Shaded band is the Bayesian (Bchron) 95 % confidence uncertainty envelope of the U-Pb age model. Fm–Formation.

3.3. Cyclostratigraphy

High resolution (5-cm spacing) elemental scanning by portable X-ray fluorescence (pXRF) was used to examine Milankovitch cyclicity of the Jiufotang Formation in core YSDP-1. The Fe/Al ratio was selected as a paleoclimate proxy. Correlation Coefficient (COCO) analyses indicate an optimal sedimentation rate of 8–12 cm/kyr, with the significance level of the null hypothesis of no orbital forcing being <0.001 (Fig. 4a). This result is consistent with the U-Pb geochronological estimate of ~8.5 cm/kyr calculated between the core top (121.09 Ma, 0 m) and CYZK-41 (124.44 ± 0.29 Ma, 283.73 m). Power spectral analysis reveals significant periods of 38 m, 8–12 m, 3–4.7 m, and 1.7–2.4 m wavelengths (Fig. 4b). These wavelengths may represent the 405 kyr long eccentricity, ~100 kyr short eccentricity, ~37 kyr obliquity, and ~20 kyr precession cycles, respectively, based on the COCO-derived sedimentation rates of 8–12 cm/kyr (Fig. 4b). Leveraging the stability of the 405-kyr eccentricity cycle during the Mesozoic (Laskar et al., 2011), a floating astronomical timescale was established by tuning the filtered 38 m cycles to match the 405 kyr periodicity (Fig. 4c).

3.4. Radioisotopically anchored astrochronology

The astrochronological framework agrees closely with U-Pb geochronology. First, the stratigraphic interval between tuff layers CYZK-16 (121.258 ± 0.043 Ma) and CYZK-22 (122.505 ± 0.088 Ma) encompasses three 405-kyr long eccentricity cycles (E2–E4; Fig. 4c). This astrochronological estimate corresponds to a duration of ~1.22 Myr, which is statistically consistent with the geochronologically derived interval of 1.25 ± 0.10 Myr between the two dated horizons. Second, the sequence from CYZK-22 to CYZK-41 (124.44 ± 0.29 Ma) contains about 4 long eccentricity cycles (E5–E8; Fig. 4c), in agreement with the radiometric duration of 1.94 ± 0.30 Myr.

The close agreement between the astrochronological and U-Pb derived durations (within method uncertainties) supports the robustness of the chronostratigraphic framework. The floating astronomical timescale was anchored at 122.505 ± 0.088 Ma (CYZK-22, mid-sequence) and 121.258 ± 0.043 Ma (CYZK-16, upper succession) (Fig. 4c). Accordingly, eight 405 kyr long eccentricity cycles (E1–E8) were identified within the 274.4–8.4 m interval, spanning from 123.86 to 120.77 Ma (Fig. 4c).

3.5. Organic carbon isotope

M.D. Sun et al. (2025) reported $\delta^{13}C_{org}$ data from 717 samples of the YSDP-4 core, ranging from −19.29 ‰ to −29.79 ‰. For this study, we conducted high-resolution sampling from the 1280–1330 m interval of YSDP-4, collecting 24 additional samples that yielded $\delta^{13}C_{org}$ values ranging from −22.42 ‰ to −32.40 ‰ (Figure 2d; Table S2).

4. Discussion

4.1. Previous geochronological constraints on the Jiufotang formation

Previous geochronological studies have tentatively constrained the depositional duration of the Jiufotang Formation in western Liaoning to ~3 Myr (122–119 Ma; Table S3). However, the lack of direct age constraints at both the basal and upper boundaries has hindered a precise estimation of its full temporal extent. The first radiometric date (110.59 ± 0.52 Ma) was obtained from an intrusive basalt dyke in Inner Mongolia (Eberth et al., 1993), providing only a minimum constraint. Subsequent studies in the Chaoyang Basin have yielded critical geochronological references. For instance, a fossil-bearing tuff from the Shangheshou section yielded a $^{40}Ar/^{39}Ar$ age of 120.3 ± 0.7 Ma (He et al. 2004), subsequently recalculated to 121.10 ± 0.70/1.10 Ma (Yu et al., 2021). Further efforts have produced LA-ICP-MS U-Pb ages from the middle Jiufotang Formation ranging from 121.06 ± 0.63 Ma to 119.72 ± 0.40 Ma (Li et al., 2023), and a CA-ID-TIMS U-Pb age of 121.272 ± 0.040 Ma from its upper part (Zhang et al., 2025). In the Jianchang Basin, SIMS U-Pb ages range from 122.0 ± 0.9 Ma at the base to 118.6 ± 1.1 Ma at the top (Yu et al., 2021). In the Fuxin-Yixian Basin, Chang et al. (2009) reported an $^{40}Ar/^{39}Ar$ age of 122.1 ± 0.3 Ma from a tuff at the lowermost part of the formation, while Ying et al. (2025) obtained a LA-ICP-MS U-Pb age of 118.07 ± 0.98 Ma. Despite these advances, none of these studies have directly constrained the basal or upper boundaries of the formation, and conflicting ages from correlative horizons highlight persistent uncertainties. For example, sample JC17–3 in this study is dated at 121.539 ± 0.085 Ma, yet it comes from the same horizon as sample XTZ17–2, which Yu et al. (2021) dated at 118.8 ± 0.6 Ma, that is ~3.0 Myr younger than the CA-ID-IRMS U-Pb age of JC17–3 in this study. The results suggest that the Jehol fossils from the Xiaotaizi section may be contemporaneous with, or even predate, those from the Shanghesho section in the Chaoyang Basin. Since both sites have yielded significant vertebrate fossils, this revised chronological framework is crucial for refining the evolutionary timeline of the Jehol Biota.

Recent analyses from the YSDP-4 core in the Kazuo Basin suggests a drastically longer depositional interval of ~9 Myr (121.36–112.25 Ma) for the Jiufotang Formation (M.D. Sun et al., 2025). However, this estimate lacks a direct basal constraint because the core did not penetrate the base of the formation. Collectively, these issues underscore a fundamental limitation in existing age models, which currently suggest durations ranging from 3 Myr to 9 Myr due to the absence of unequivocal boundary dates.

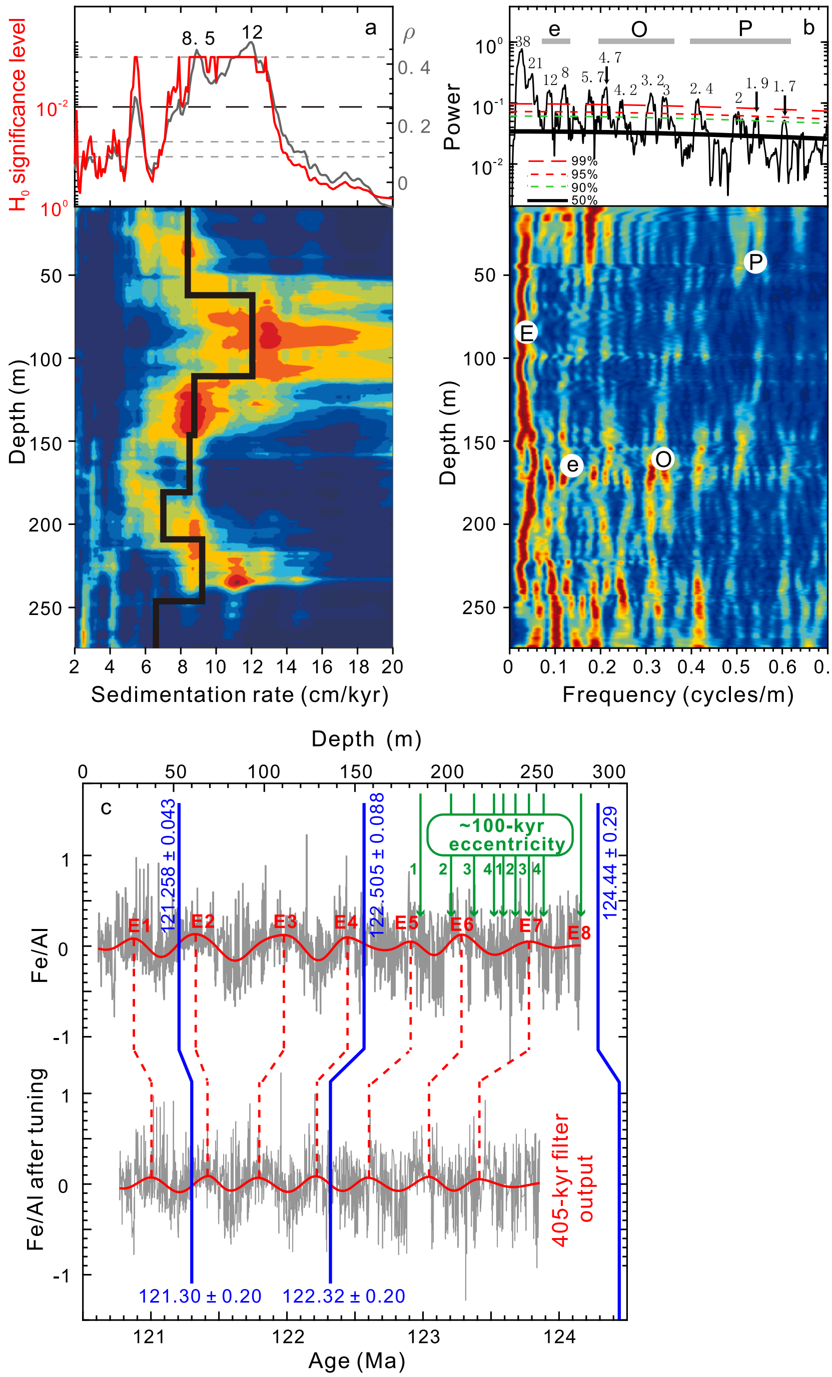

Fig. 4. (a) COCO analysis (top) and evolutionary correlation coefficient (eCOCO) sedimentation rate map (bottom, colored area; red, peaks; blue, valleys) of the Fe/Al series after removing a 100 m 'loess' trend. Black line shows sedimentation rate variation based on 405 kyr tuning of 38 m cycles. (b) Power spectrum (top) and evolutionary spectral analysis (bottom, colored area; red, peaks; blue, valleys) of the Fe/Al series from the Jiufotang Formation in the YSDP-1 core. For both the COCO and eCOCO analyses, tested sedimentation rate range is set to 2–20 cm/kyr, with a step of 0.1 cm/kyr, and the number of Monte Carlo simulations is 2000; the sliding window is 57 m. E, e, O, and P indicate long eccentricity, short eccentricity, obliquity, and precession terms, respectively. (c) Detrended Fe/Al series (grey) are plotted with filtered 405 kyr cycles (red, Guass filter, passbands are 0.0263 ± 0.008 cycles/m and 0.002469 ± 0.0007 cycles/kyr in the stratigraphic (top) and time (bottom) domains, respectively).

4.2. Duration of the Jiufotang formation and temporal constraints on the late phase of the Jehol Biota

New chronostratigraphic data from the YSDP-1 and YSDP-4 cores allow for a refined estimate of the duration of the Jiufotang Formation. The YSDP-1 core penetrates the underlying Yixian Formation, thereby directly constraining the basal boundary of the Jiufotang Formation. This boundary is marked by sample CYZK-41 (124.44 ± 0.29 Ma), consistent with the termination age of the Yixian Formation within uncertainties (124.122 ± 0.048 Ma; Zhong et al., 2021). Additionally, CYZK-45 (306.14–306.27 m) yields an age of 125.505 ± 0.047 Ma, confirming that volcanic rocks below 284.46 m in YSDP-1 belong to the Yixian Formation.

Organic carbon isotope composition ($\delta^{13}C_{org}$) was used to correlate YSDP-1 and YSDP-4 stratigraphy (Fig. 2d). Both cores exhibit synchronous $\delta^{13}C_{org}$ excursions: in YSDP-4 (1335–1279 m), values decline from

−24.3 ‰ to −28.8 ‰ before abruptly rising to −22.6 ‰; in YSDP-1 (63–14 m), $\delta^{13}C_{org}$ decreases from −21.5 ‰ to −28 ‰, followed by a rebound to −23.4 ‰ (Fig. 2d). Therefore, these comparable patterns, support by consistent geochronological constraints, indicate that the upper part of YSDP-1 (63–14 m) overlaps in time with the lower portion of YSDP-4 (1335–1279 m) (Fig. 2d). Thus, their age frameworks can be integrated. The more condensed appearance of the YSDP-1 profile mainly reflects its marginal position in the Chaoyang Basin compared with the more central position of YSDP-4 in the Kazuo Basin, although the sedimentation rates of the two intervals (8–10 cm/kyr vs. 16.6 cm/kyr) remain broadly comparable. Combining these data, we constrain the Jiufotang Formation to a duration of ~12.2-Myr (124.44–112.25 Ma), spanning the Early Barremian to the Early Albian. This new estimate contrast with earlier estimates of ~3 Myr (~122–119 Ma) or ~9 Myr (121.36–112.25 Ma), which lacked direct age control at formation boundary. Unlike previous studies that relied solely on intra-formational radiometric dates (e.g., Li et al., 2023), our study combines a direct basal boundary age from the YSDP-1 with high-resolution $\delta^{13}C_{org}$ chemostratigraphic correlation between YSDP-1 and YSDP-4 cores.

We correlate the top of the YSDP-1 core with the tuff horizon of the Shangheshou section (see Section 2). And our Bayesian-model-derived age for the top of the YSDP-1 core (121.09+0.18/−0.75 Ma) closely matches the age of the Shangheshou section (121.10 ± 0.70/1.10 Ma; Yu et al., 2021), a key fossil-bearing horizon long used to mark the end of the Jehol Biota (Zhou, 2006; Zhou et al., 2021). Consequently, the late stage of Jehol Biota (i.e., JBS III) is now constrained to ~124–121 Ma, narrowing its previously estimated duration by 1 Myr. This refined time frame further highlights the rapid diversification and remarkable differentiation of the JBS III (Zhou et al., 2021) and suggests that its evolutionary radiation may have been more rapid than previously assumed. Importantly, while the Jiufotang Formation spans ~12.2 Myr, this extended duration cannot be taken as equivalent to the temporal range of the late stage of the Jehol Biota, which is confined to ~124–121 Ma.

4.3. Implications on the role of tectonic-volcanic-climatic interaction in evolution of the Jehol Biota

Northeast China experienced significant destruction of the North China Craton during the Early Cretaceous (Wu et al., 2019; Zhu and Xu, 2019). This period was marked by lithospheric thinning and asthenospheric upwelling, which drove the transition from compressional foreland to extensional rift settings (Meng et al., 2022). The extensional tectonic regime promoted the development of rift basins and freshwater lakes, which hosted the deposition of the Yixian and Jiufotang formations, thereby preserving the JBS II and III (Zhou, 2014). An 11.2 m fossils-bearing succession in the Yixian Formation at the Sihetun Museum section records a low sedimentation rate of ~1.7 cm/kyr (Wu et al., 2013). Li et al. (2022) further anchored the astrochronology of Wu et al. (2013) with $^{40}Ar/^{39}Ar$ ages, yielding average rates of ~1.8–2.4 cm/kyr (up to ~3.8 cm/kyr with uncertainties), and these values are consistent with earlier independent estimates using palaeomagnetic methods (Zhu et al., 2007). By contrast, MacLennan et al. (2024) reported a much higher rate (~137 cm/kyr) from a ~90 m core interval at Huangbanjigou. These different values are not contradictory but instead reflect alternating episodes of rapid and slower deposition. Using the total duration of the Yixian Formation (125.882–124.122 Ma; Zhong et al., 2021; MacLennan et al., 2024) and the ~289 m sedimentary interval in the type section at Mashenmiao-Songbahu (Zhang et al., 2004) yields a rate of ~16 cm/kyr. This represents only a rough minimum estimate of the average rate for the Yixian Formation. Taken together, these observations show that sedimentation rates within the Yixian Formation were highly variable both spatially and temporally. This variability was likely controlled by volcanism, sediment supply, and basin setting, and may reflect deposition in small and scattered lakes (Zhou et al., 2016). Future work is needed to better constrain this variability.

In contrast, the Jiufotang Formation is composed almost entirely sedimentary with interbedded ashes. Core data (YSDP-1 and YSDP-4; M. D. Sun et al., 2025; this study) show sedimentation rates of 8–16 cm/kyr, reflecting a relatively stable setting with sustained subsidence. These conditions promoted the expansion of large lakes and shaped the habitats in which the Jehol Biota thrived.

Volcanic activity strongly influenced lacustrine environments during Jehol time. Volcanic ash layers preserved in both YSDP-1 (~1–155.2 m) and YSDP-4 (~850–1497.4 m) cores reveal frequent explosive volcanism between ~122.5 Ma and 117.4 Ma. These eruptions not only supplied abundant ashes but also nutrients that enhanced primary productivity, producing organic-rich intervals. Associated eutrophication may have led to bottom-water anoxia, while eruption-induced seismicity caused water column mixing and transient oxygenation (Cai et al., 2023, 2025). These fluctuating redox conditions, together with rapid burial, facilitated exceptional fossil preservation in the Jiufotang Formation. However, the absence of Konservat-Lagerstätten above the ~121.1 Ma horizon implies that volcanism alone cannot explain fossil preservation. Other factors, such as the evolutionary stage of biota and its habitats, also played important roles, though further investigations are needed.

Climate perturbations further shaped the ecological and depositional framework. The Aptian cold interval occurred within the broader Early Cretaceous greenhouse context and reflects complex interactions among volcanic CO_2 emissions, organic carbon burial, and silicate weathering (Jenkyns, 2018). Black shale intervals in both cores document enhanced lake productivity and widespread carbon burial, highlighting global carbon cycle perturbations (Cai et al., 2023, 2025; Sun M et al., 2025a; Sun Z et al., 2025b). Declining volcanic CO_2 inputs and increased carbon burial collectively acted as major CO_2 sinks, driving climatic cooling. Palynological data document a two-phase Aptian cooling: an initial moderate phase (~117.5–114 Ma) followed by a more pronounced phase from ~114 to 112 Ma (Lu et al., 2025). Together, the Jiufotang Formation records a dynamic system in which tectonic processes modulated basin development, volcanism influenced nutrient cycling and redox conditions, and climate perturbations imposed selective pressures on ecosystems. These interconnected deep earth-surface processes provide key insights into how Jehol Biota evolved under coupled tectonic, volcanic, and climatic forces.

5. Conclusion

Our integrated study of the YSDP-1 core from the Early Cretaceous Jiufotang Formation, combining high-precision U-Pb geochronology, Bayesian age modeling, and cyclostratigraphy, yields the following conclusions:

(1) The boundary of the Yixian/Jiufotang formations in the Chaoyang Basin is dated at 124.44 ± 0.29 Ma, providing a direct and reliable constraint on the onset of the Jiufotang Formation.

(2) Correlative $\delta^{13}C_{org}$ excursions across different basins serve as reliable chemostratigraphic markers. The Jiufotang Formation in western Liaoning is constrained to a depositional interval of ~12.2 Myr, from 124.44 ± 0.29 Ma to 112.25 Ma, spanning the Early Barremian to Early Albian.

(3) High-precision age constraints for exceptionally preserved fossiliferous layers help resolve temporal correlations among basins. The Shangheshou section in the Chaoyang Basin yields an age of 121.09+0.18/−0.75 Ma, while the Xiaotaizi section in the Jianchang Basin dates to 121.539 ± 0.085/0.093/0.272 Ma. These results indicate that Jehol Biota fossils from Xiaotaizi are either contemporaneous with or slightly older than those from Shangheshou. Consequently, the duration of Jehol Biota Stage III is now refined to ~124–121 Ma, shortening previously estimates by ~1 Myr and highlighting the rapid diversification during its late phase.

(4) Sedimentation in the Jiufotang Formation was relatively stable at

8–16 cm/kyr, reflecting sustained rift-related subsidence during the destruction of the North China Craton. The interplay of volcanism, continuous sediment accumulation, and fluctuating redox conditions created depositional environments conducive to the exceptional fossil preservation in the Jiufotang Formation.

Supplemental material

The supplementary information includes Supplementary Text, Figures S1 and S2, and Tables S1 to S3.

CRediT authorship contribution statement

Yu-Ting Zhong: Writing – review & editing, Writing – original draft, Visualization, Validation, Software, Resources, Methodology, Investigation, Funding acquisition, Data curation, Conceptualization. **Magdalena H. Huyskens:** Writing – review & editing, Methodology, Data curation. **Run-Jian Chu:** Writing – review & editing, Writing – original draft, Visualization, Validation, Software, Methodology, Data curation. **Han-Qing Yang:** Methodology, Data curation. **Jian-Fang Hu:** Writing – review & editing, Methodology, Investigation, Data curation. **Ya-Qiong Wang:** Writing – review & editing, Writing – original draft, Resources, Investigation. **Shi-Xi Cai:** Writing – review & editing, Investigation, Data curation. **Qiong Wu:** Visualization, Software, Methodology, Investigation. **Qiang Ma:** Writing – review & editing, Resources, Investigation. **Huai-Chun Wu:** Writing – review & editing, Visualization, Validation, Software, Methodology, Investigation, Data curation. **Qing-Zhu Yin:** Writing – review & editing, Methodology, Investigation, Data curation. **Yi-Gang Xu:** Writing – review & editing, Supervision, Resources, Project administration, Investigation, Funding acquisition, Conceptualization.

Declaration of competing interest

The authors declare no competing interests.

Acknowledgements

This work was supported by the National Science Foundation of China (42288201, 42372022 and 41873018) and Funding by Science and Technology Projects in Guangzhou (SL2024A04J01863). We thank the Chaoyang Bird Fossil National Geological Park for permission to conduct drilling near the fossil excavation site. Thanks to YSDP team members for their assistance with sample collection and pXRF measurements. We thank Profs. Xiaolin Wang, Jun Shen, and Mingdao Sun for the valuable discussions. We also thank Editor Alex Webb, Scott MacLennan, and an anonymous reviewer for their constructive comments and suggestions. This is contribution No.IS-3717 from GIGCAS.

Supplementary materials

Supplementary material associated with this article can be found, in the online version, at doi:10.1016/j.epsl.2025.119688.

Data availability

Data will be made available on request.

References

Cai, S., Wei, G., Hu, J., Zeng, T., Xu, Y.-G., 2025. Influence of tectono-volcanism on the depositional environment of the early cretaceous Jiufotang Formation in western Liaoning — a case study of Yanshan Scientific Drilling Project borehole (YSDP-1). Geochimica. https://doi.org/10.19700/j.0379-1726.2024.01.101. Chinese with English abstract.

Cai, S., Wei, G., Lo, L., Hu, J., Sun, Z., Zeng, T., Wei, Y., Zhou, Z.H., Xu, Y.-G., 2023. Volcanism-driven lacustrine redox fluctuations were responsible for the formation of the Jehol Lagerstätte: evidence from a high-resolution Aptian sedimentary core, Northeast China. Palaeogeogr. Palaeoclimatol. Palaeoecol. 631, 111833. https://doi.org/10.1016/j.palaeo.2023.111833.

Chang, S.-C., Zhang, H., Renne, P.R., Fang, Y., 2009. High-precision $^{40}Ar/^{39}Ar$ age for the Jehol Biota. Palaeogeogr. Palaeoclimatol. Palaeoecol. 280 (1–2), 94–104. https://doi.org/10.1016/j.palaeo.2009.06.021.

Eberth, D.A., Russell, D.A., Braman, D.R., Deino, A.L., 1993. The age of the dinosaur-bearing sediments at Tebch, Inner Mongolia, People's Republic of China. Can. J. Earth Sci. 30 (10), 2101–2106. https://doi.org/10.1139/e93-182.

Haslett, J., Parnell, A., 2008. A simple monotone process with application to radiocarbon-dated depth chronologies. J. Royal Statist. Soc.: Series C (Applied Statistics) 57 (4), 399–418. https://doi.org/10.1111/j.1467-9876.2008.00623.x.

He, H.Y., Wang, X.L., Zhou, Z.H., Wang, F., Boven, A., Shi, G.H., Zhu, R.X., 2004. Timing of the Jiufotang Formation (Jehol Group) in Liaoning, northeastern China, and its implications. Geophys. Res. Lett. 31, L12605. https://doi.org/10.1029/2004GL019790.

Jenkyns, H.C., 2018. Transient cooling episodes during cretaceous Oceanic Anoxic Events with special reference to OAE 1a (Early Aptian). Philosoph. Transac. Royal Soc. A: Math., Phy. Eng. Sci. 376 (2130), 20170073. https://doi.org/10.1098/rsta.2017.0073.

Jiang, B., Sha, J., 2006. Late mesozoic stratigraphy in western Liaoning, China: a review. J. Asian Earth Sci. 28 (4–6), 205–217. https://doi.org/10.1016/j.jseaes.2005.07.006.

Laskar, J., Fienga, A., Gastineau, M., Manche, H., 2011. La2010: a new orbital solution for the long-term motion of the Earth. Astro. Astrophy. 532, A89.

Li, L., He, W., Liu, Z., Song, Y., Li, Y., Belousova, E., Löhr, S.C., George, S.C., 2023. Volcanic activity drives lacustrine carbon sequestration after Oceanic Anoxic Event 1a. Palaeogeogr. Palaeoclimatol. Palaeoecol. 621, 111595. https://doi.org/10.1016/j.palaeo.2023.111595.

Li, Y., Jicha, B.R., Yu, Z., Wu, H., Wang, X., Singer, B.S., He, H., Zhou, Z., 2022. Rapid preservation of jehol biota in Northeast China from high precision $^{40}Ar/^{39}Ar$ geochronology. Earth Planet. Sci. Lett. 594, 117718. https://doi.org/10.1016/j.epsl.2022.117718.

Lu, C., Lin, M.Q., Shen, J., Ji, X.K., Yang, C.M., Zhang, Z.H., He, Q., Sun, M.D., Xu, Y.-G., 2025. A continental record of early cretaceous (Aptian) vegetation and climate change based on palynology and clay mineralogy from the North China Craton. Palaeogeogr. Palaeoclimatol. Palaeoecol., 112750 https://doi.org/10.1016/j.palaeo.2025.112750.

MacLennan, S.A., Sha, J., Olsen, P.E., Kinney, S.T., Chang, C., Fang, Y., Liu, J., Slibeck, B. B., Chen, E., Schoene, B., 2024. Extremely rapid, yet noncatastrophic, preservation of the flattened-feathered and 3D dinosaurs of the early Cretaceous of China. Proceed. Nat. Acad. Sci. 121 (47), e2322875121. https://doi.org/10.1073/pnas.2322875121.

Meng, Q., Zhou, Z., Zhu, R., Xu, Y.-G., Guo, Z., 2022. Cretaceous basin evolution in northeast Asia: tectonic responses to the paleo-Pacific plate subduction. Natl. Sci. Rev. 9, nwab088. https://doi.org/10.1093/nsr/nwab088.

Meng, X., 2008. A New Species of *Sinopterus* from Jehol Biota and Reconstruction of Stratigraphic Sequence of the Jiufotang Formation (Master's Thesis). Graduate University of Chinese Academy of Sciences, Beijing, p. 57.

Parnell, A.C., Haslett, J., Allen, J.R., Buck, C.E., Huntley, B., 2008. A flexible approach to assessing synchroneity of past events using bayesian reconstructions of sedimentation history. Quat. Sci. Rev. 27 (19–20), 1872–1885. https://doi.org/10.1016/j.quascirev.2008.07.009.

Sha, J.G., 2007. Cretaceous stratigraphy of Northeast China: non-marine and marine correlation. Cretac. Res. 28 (1), 146–170. https://doi.org/10.1016/j.cretres.2006.12.002.

Sun, M.D., Lin, Q., Ramezani, J., Liu, J.S., Lu, Z.A., Yang, H.Q., 2025a. Terrestrial ecosystem response to early cretaceous global environmental change: a calibrated, high-resolution Aptian record from Northeast China. Earth Planet. Sci. Lett. 653, 119206. https://doi.org/10.1016/j.epsl.2025.119206.

Sun, Z., Cai, S., Hu, J., 2025b. Lacustrine records of large amounts of organic carbon burial in the early cretaceous period: a case study of the Jiufotang formation in the Chaoyang Basin. Geochimica. https://doi.org/10.19700/j.0379-1726.2024.01.115. Chinese with English abstract.

Swisher, C.C., Wang, X., Zhou, Z., Wang, Y., Jin, F., Zhang, J., Xu, X., Zhang, F., Wang, Y., 2002. Further support for a cretaceous age for the feathered-dinosaur beds of Liaoning, China: new $^{40}Ar/^{39}Ar$ dating of the Yixian and Tuchengzi formations. Chin. Sci. Bull. 47 (2), 136–139.

Wu, F.Y., Yang, J.H., Xu, Y.G., Wilde, S.A., Walker, R.J., 2019. Destruction of the North China craton in the Mesozoic. Annu. Rev. Earth Planet Sci. 47 (1), 173–195. https://doi.org/10.1146/annurev-earth-053018-060342.

Wu, H., Zhang, S., Jiang, G., Yang, T., Guo, J., Li, H., 2013. Astrochronology for the early cretaceous Jehol Biota in northeastern China. Palaeogeogr. Palaeoclimatol. Palaeoecol. 385, 221–228. https://doi.org/10.1016/j.palaeo.2013.05.017.

Yang, S., He, H., Jin, F., Zhang, F., Wu, Y., Yu, Z., Li, Q.L., Wang, M., O'Connor, J.K., Deng, C., Zhu, R.X., Zhou, Z., 2020. The appearance and duration of the Jehol Biota: constraint from SIMS U-Pb zircon dating for the Huajiying Formation in northern China. Proceed. Nat. Acad. Sci. 117 (25), 14299–14305. https://doi.org/10.1073/pnas.191827211.

Ying, Q., Sun, S., Zhang, D., Liang, F., Feng, Y., Wang, G., Wang, S., Bugdaeva, E., Markevich, V., Popa, M.E., 2025. New palynological data and U–Pb dating from the Jiufotang Formation: implications for the late Jehol Biota. Rev. Palaeobot. Palynol. 334, 105270. https://doi.org/10.1016/j.revpalbo.2024.105270.

Yu, Z., Wang, M., Li, Y., Deng, C., He, H., 2021. New geochronological constraints for the lower cretaceous Jiufotang Formation in Jianchang Basin, NE China, and their

implications for the late Jehol Biota. Palaeogeogr. Palaeoclimatol. Palaeoecol. 583, 110657. https://doi.org/10.1016/j.palaeo.2021.110657.
Zhang, H., Wang, W., Li, Z., Yang, F., 2004. Comprehensive correlation of the Yixian Formation in the Beipiao and Yixian areas, western Liaoning. Geol. Bull. China 23 (8), 766–777. Chinese with English abstract.
Zhang, L.J., Song, S.Y., Ji, S.A., Chang, S.C., Ramezani, J., Gao, F., Wang, B., Zhang, H., Zheng, D.R., 2025. High-precision age constraint for the Xiyingzi Bed of the Jiufotang Formation in western Liaoning, Northeast China. Palaeoworld 34 (4), 100901. https://doi.org/10.1016/j.palwor.2024.11.009.
Zhong, Y., Huyskens, M.H., Yin, Q.Z., Wang, Y., Ma, Q., Xu, Y.G., 2021. High-precision geochronological constraints on the duration of 'Dinosaur Pompeii' and the Yixian Formation. Natl. Sci. Rev. 8 (6). https://doi.org/10.1093/nsr/nwab063 nwab063.
Zhou, L., Algeo, T.J., Feng, L., Zhu, R., Pan, Y., Gao, S., Zhao, L.S., Wu, Y., 2016. Relationship of pyroclastic volcanism and lake-water acidification to Jehol Biota mass mortality events (Early Cretaceous, northeastern China). Chem. Geol. 428, 59–76. https://doi.org/10.1016/j.chemgeo.2016.02.029.
Zhou, Z., 2006. Evolutionary radiation of the Jehol Biota: chronological and ecological perspectives. Geol. J. 41 (3–4), 377–393. https://doi.org/10.1002/gj.1045.
Zhou, Z., 2014. The Jehol Biota, an early cretaceous terrestrial lagerstätte: new discoveries and implications. Natl. Sci. Rev. 1 (4), 543–559. https://doi.org/10.1093/nsr/nwu055.
Zhou, Z., Barrett, P.M., Hilton, J., 2003. An exceptionally preserved Lower Cretaceous ecosystem. Nature 421 (6925), 807–814. https://doi.org/10.1038/nature01420.
Zhou, Z., Meng, Q., Zhu, R., Wang, M., 2021. Spatiotemporal evolution of the Jehol Biota: responses to the North China craton destruction in the early Cretaceous. Proceed. Nat. Acad. Sci. 118 (34), e2107859118. https://doi.org/10.1073/pnas.2107859118.
Zhu, R., Xu, Y.G., 2019. The subduction of the west Pacific plate and the destruction of the North China Craton. Sci. China Earth Sci. 62 (9), 1340–1350. https://doi.org/10.1007/s11430-018-9356-y.
Zhu, R., Pan, Y., Shi, R., Liu, Q., Li, D., 2007. Palaeomagnetic and $^{40}Ar/^{39}Ar$ dating constraints on the age of the Jehol Biota and the duration of deposition of the Sihetun fossil-bearing lake sediments, northeast China. Cretac. Res. 28 (2), 171–176. https://doi.org/10.1016/j.cretres.2006.06.003.